Kinetics and Mechanism of Reversible Oxidative Addition of Hydrogen across the Metal−Metal Bond of $(\mu\text{-H})_2Ru_3(CO)_8(\mu\text{-P}(t\text{-Bu})_2)_2$. Steric Promotion of Metal−Metal Bond Cleavage But a CO Dissociative Mechanism

Fred J. Safarowic, David J. Bierdeman, and Jerome B. Keister*

Contribution from the Department of Chemistry, University at Buffalo, The State University of New York at Buffalo, Buffalo, New York 14260-3000

Received August 16, 1996[⊗]

Abstract: The kinetics of the reaction $(\mu\text{-H})_2Ru_3(CO)_8(\mu\text{-P}(t\text{-Bu})_2)_2 + H_2 \rightleftarrows (\mu\text{-H})_2Ru_3(CO)_8(H)_2(\mu\text{-P}(t\text{-Bu})_2)_2$ have been studied. The reaction of $(\mu\text{-H})_2Ru_3(CO)_8(\mu\text{-P}(t\text{-Bu})_2)_2$ with H_2 has a rate law which is first-order in cluster concentration and in hydrogen pressure and inverse order in CO pressure; on the basis of the rate law, activation parameters, and deuterium kinetic isotope effect, hydrogen addition is proposed to involve rapid, reversible dissociation of a carbonyl ligand, followed by rate-determining oxidative addition of hydrogen through a three-center transition state at a single metal atom. Loss of hydrogen from $(\mu\text{-H})_2Ru_3(H)_2(CO)_8(\mu\text{-P}(t\text{-Bu})_2)_2$ also involves reversible loss of a carbonyl, followed by rate-determining reductive elimination of molecular hydrogen. The reaction is highly sensitive to the steric bulk of the phosphido substituents, as $(\mu\text{-H})_2Ru_3(CO)_8(\mu\text{-PR}_2)_2$, R = cyclohexyl and phenyl, do not react with hydrogen. In addition, the rate of exchange with ^{13}CO is much faster for R = *t*-Bu than for R = cyclohexyl. Based upon the temperature dependence of the equilibrium constant for hydrogenation, the energy for the unbridged Ru−Ru bond of $(\mu\text{-H})_2Ru_3(CO)_8(\mu\text{-P}(t\text{-Bu})_2)_2$ is estimated to be 47−59 kJ/mol, the low value being attributed to steric strain.

Introduction

The oxidative addition of hydrogen to a transition metal center is one of the most fundamental reactions of organotransition metal chemistry and is a key step in metal catalyzed hydrogenations.[1] Numerous studies have focused upon the mechanism of hydrogen addition to a single metal center, which is proposed to involve a three-center, synchronous addition.[2] Other mechanisms are heterolytic cleavage[3] or homolytic cleavage[4] to form two monometallic monohydrides.

Metal cluster reactions and their mechanisms are of interest due to the possible involvement of two or more metal atoms in the activation step. A few studies of the kinetics of H_2 addition to and/or elimination from clusters of two or more metal atoms have been reported.[5−12] In most of these hydrogen addition follows rate-determining loss of a ligand, while rate-determining hydrogen elimination is followed by addition of a two-electron donor ligand. Although in almost all cases the hydride ligands involved in the reaction bridge two metal centers, the elimination/addition step has been proposed to occur at a single metal center.

In 1988 Jones et al. described the reaction of hydrogen with $(\mu\text{-H})_2Ru_3(CO)_8(\mu\text{-P}(t\text{-Bu})_2)_2$, in which addition occurs quantitatively and reversibly across an unbridged metal−metal bond, producing $(\mu\text{-H})_2Ru_3(H)_2(CO)_8(\mu\text{-P}(t\text{-Bu})_2)_2$ (Figure 1).[13] The reaction is of interest as one of the few examples of (1) addition of hydrogen across a metal−metal bond, especially a single bond, and (2) formation and elimination of two terminal hydrides on a cluster. We report here a study of the kinetics and mechanism of this novel reaction.

Experimental Section

The clusters $(\mu\text{-H})_2Ru_3(CO)_8(\mu\text{-PPh}_2)_2$[14] and $(\mu\text{-H})_2Ru_3(CO)_8(\mu\text{-P}(t\text{-Bu})_2)_2$[13] were prepared by previously reported methods. All solvents were used as received from Aldrich Chemical Co., Inc. Gases and

[⊗] Abstract published in *Advance ACS Abstracts,* November 1, 1996.

(1) (a) Collman, J. P.; Hegedus, L. S.; Norton, J. R.; Finke, R. G. Principles and Applications of Organotransition Metal Chemistry; University Science Books: Mill Valley, CA, 1987; Chapter 5. (b) James, B. R. Homogeneous Hydrogenation; Wiley: New York, 1973. (c) James, B. R. In Comprehensive Organometallic Chemistry; Wilkinson, G., Stone, F. G. A., Abel, E., Eds.; Pergamon: Oxford, 1982; Vol. 8, Chapter 51.

(2) General reviews are given in ref 1. A representative set of significant and leading references for the three-center mechanism is: (a) Chock, P. B.; Halpern, J. *J. Am. Chem. Soc.* **1966**, *88*, 3511. (b) Obara, S.; Kitaura, K.; Morokuma, K. *J. Am. Chem. Soc.* **1984**, *106*, 7482. (c) Johnson, C. E.; Eisenberg, R. *J. Am. Chem. Soc.* **1985**, *107*, 3148. (d) Zhou, P.; Vitale, A. A.; San Filippo, J., Jr.; Saunders, W. H., Jr. *J. Am. Chem. Soc.* **1985**, *107*, 8049. (e) Low, J. J.; Goddard, W. A., III *Organometallics* **1986**, *5*, 609. (f) Burk, M. J.; McGarth, M. P.; Wheeler, R.; Crabtree, R. H. *J. Am. Chem. Soc.* **1988**, *110*, 5034. A general reference concerning molecular hydrogen complexes is: Heinekey, D. M.; Oldham, W. J., Jr. *Chem. Rev.* **1993**, *93*, 913.

(3) Brothers, P. J. *Prog. Inorg. Chem.* **1981**, *28*, 1.

(4) Halpern, J. *Inorg. Chim. Acta* **1982**, *62*, 31.

(5) (a) Bavaro, L. M.; Montangero, P.; Keister, J. B. *J. Am. Chem. Soc.* **1983**, *105*, 4977. (b) Anhaus, J.; Bajaj, H. C.; van Eldik, R.; Nevinger, L. R.; Keister, J. B. *Organometallics* **1989**, *8*, 2903. (c) Bavaro, L. M.; Keister, J. B. *J. Organometal. Chem.* **1985**, *287*, 357. (d) Keister, J. B.; Onyeso, C. C. O. *Organometallics* **1988**, *7*, 2364.

(6) Nevinger, L. R.; Keister, J. B.; Maher, J. *Organometallics* **1990**, *9*, 1900.

(7) (a) Poë, A. J.; Sampson, C. N.; Smith, R. T.; Zheng, Y. *J. Am. Chem. Soc.* **1993**, *115*, 3174. (b) Hudson, R. H. E.; Poë, A. J.; Sampson, C. N.; Siegel, A. *J. Chem. Soc., Dalton Trans.* **1989**, 2235.

(8) Doi, Y.; Koshizuka, K.; Keii, T. *Inorg. Chem.* **1982**, *21*, 2732.

(9) Taube, D. J.; Rokicki, A.; Anstock, M.; Ford, P. C. *Inorg. Chem.* **1987**, *26*, 526.

(10) Garland, M.; Pino, P. *Organometallics* **1990**, *9*, 1943.

(11) Casey, C. P.; Hallenbeck, S. L.; Widenhoefer, R. A. *J. Am. Chem. Soc.* **1995**, *117*, 4607.

(12) Hallen, R. T.; Hubler, T. L.; Lilga, M. A. Abstracts of Papers; 207th National Meeting of the American Chemical Society; San Diego, CA, March 13−17, 1994; American Chemical Society: Washington, DC, 1994; INOR 185.

(13) Arif, A. M.; Bright, T. A.; Jones, R. A.; Nunn, C. M. *J. Am. Chem. Soc.* **1988**, *110*, 6894.

(14) Patel, V. D.; Cherkas, A. A.; Nucciarone, D.; Taylor, N. J.; Carty, A. J. *Organometallics* **1985**, *4*, 1792.

S0002-7863(96)02881-8 CCC: $12.00

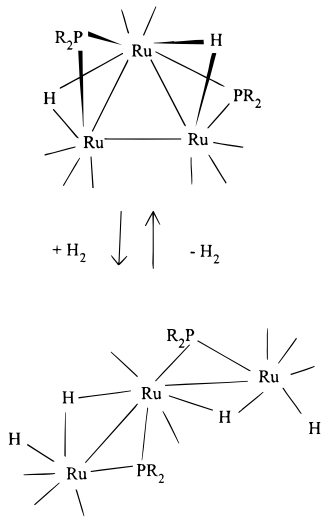

Figure 1. Reaction of (μ-H)$_2$Ru$_3$(CO)$_8$(μ-P(*t*-Bu$_2$))$_2$ with hydrogen to form (μ-H)$_2$(H)$_2$Ru$_3$(CO)$_8$(μ-P(*t*-Bu)$_2$)$_2$.

gas mixtures were either obtained from Cryogenic Supply, Buffalo, NY, or were prepared by adding CO to hydrogen, nitrogen or CO/hydrogen mixtures. Analysis of the gas composition was performed by gas chromatography for hydrogen content and IR spectroscopy for CO content. The CO component of the gas mixtures was determined by IR using a 10 cm IR gas cell. The absorbance at nine frequencies (2215.7, 2206.3, 2203.1, 2196.6, 2179.9, 2172.8, 2127.7, 2094.8, and 2059.9 cm^{-1}) were used to calculate the absorptivities (ϵ) of CO and the actual P_{CO} (atm) in each mixture. The H_2 component of each H_2/N_2 gas mixture was determined by gas chromatography using a Varian series 2700 gas chromatograph equipped with a thermal conductivity detector and a 5A 60−80 mesh molecular sieve column; it was assumed that the purchased gases contained only H_2 and N_2; therefore the N_2 component was determined by difference. Infrared spectra were recorded on a Nicolet Magna-500 FT-IR spectrometer. ^{1}H, ^{13}C, and ^{31}P NMR spectra were recorded on a Varian VXR-400 spectrometer referenced to TMS, $CDCl_3$ or *o*-phosphoric acid, respectively. UV−vis spectra were recorded on a Hewlett Packard 8452A diode array spectrophotometer fitted with a Lauda Fisher 800 isotemp constant circulating temperature cell (±0.1 °C). Mass spectra were recorded at the University at Buffalo Instrument Center on a VG 70SE spectrometer. Elemental analyses were performed by Galbraith Laboratories, Knoxville, TN. Kinetic data were determined over 2−3 half-lives in most cases and were analyzed using a variety of programs, including KINPLOT,[15] Psi-Plot (Poly Software International), and QuattroPro. Error limits are the standard errors, including the number of degrees of freedom via Student's *t* values; the 95% confidence limits can be obtained by doubling the reported uncertainties.

Kinetics for the Addition of Hydrogen. (μ-H)$_2$Ru$_3$(CO)$_8$(μ-P(*t*-Bu)$_2$)$_2$ (4 mg) was dissolved in 10 mL of heptane (0.5 mM). The sample was placed in a thermostatted UV−vis cell fitted with a septum and two syringe needles. One needle was used as a gas inlet for the appropriate gas mixture. The other needle was used to maintain a 1 atm pressure. The cell was allowed the reach thermal equilibrium (20.0, 30.0, or 40.0 °C) prior to briefly bubbling the gas through the solution at a slow rate. The gas inlet needle was then elevated to a position above the solution surface during data collection. A minimal rate of gas flow was continued throughout the data collection, in order to maintain a uniform atmosphere while minimizing heptane evaporation. Data were collected for more than 3 half-lives by monitoring the loss of the 532 nm absorption peak of the starting material. The absorption at 532 nm did not disappear completely due to the presence of a small peak at 492 nm. Therefore, plots of ln($A_t - A_\infty$), where A_t and A_∞ are the absorbances at 532 nm at times *t* and ∞, were used to determine the rate constants. The peak at 492 nm was assumed to be due to decomposition of either the starting material or the product, since a slightly higher value of the final absorbance was noted in samples that were run from recycled product. Prior to each set of runs an IR spectrum and a UV−vis spectrum were recorded for the sample.

Kinetics Determination for Hydrogen Elimination. A solution of (μ-H)$_2$Ru$_3$(CO)$_8$(μ-P(*t*-Bu)$_2$)$_2$ (12.3 mg) in heptane (10 mL, 1.5 mM) was placed in a jacketed constant temperature cell (temperature controlled (±0.1 °C) by a Haake GH constant temperature bath). The cluster was hydrogenated completely to (μ-H)$_2$Ru$_3$(H)$_2$(CO)$_8$(μ-P(*t*-Bu)$_2$)$_2$, as determined by IR spectra. The sample was then flushed with nitrogen or a carbon monoxide/nitrogen mix. The change in the IR absorption at 2081 cm^{-1} was monitored. The runs were conducted under 100% N_2 and CO/N_2 gas mixtures.

Experimental Determination of the Equilibrium Constant. (μ-H)$_2$Ru$_3$(CO)$_8$(μ-P(*t*-Bu)$_2$)$_2$ (10 mg) was dissolved in heptane (10 mL) under argon in a Schlenk flask fitted with a septum. The initial absorbance A_o at 2065.9 cm^{-1} was determined. The flask was thermostatted to the desired temperature (0−40 °C) using a Haake GH circulating bath and Haake D8 temperature controller. The flask was flushed with a gas mixture of 3.4% hydrogen in nitrogen (1 atm total pressure). An equilibrium between (μ-H)$_2$Ru$_3$(CO)$_8$(μ-P(*t*-Bu)$_2$)$_2$ and (μ-H)$_2$Ru$_3$(H)$_2$(CO)$_8$(μ-P(*t*-Bu)$_2$)$_2$ established and equilibrium absorbance A_e was measured. The equilibrium constant was determined as ($A_o - A_e$)/A_e(0.034 atm).

For the determination in THF, the IR bands were too broad to allow for quantitative determination, so the visible spectrum was monitered. A 1 mM solution of (μ-H)$_2$Ru$_3$(CO)$_8$(μ-P(*t*-Bu)$_2$)$_2$ in THF was placed in a jacketed UV cell at 30.0 °C. The absorbance A_0 at 524 nm was recorded. Then the cell was flushed with a mixture of 3.4% hydrogen in nitrogen gas (Cryogenic Supply, Buffalo, NY, certified grade) and then was sealed. After 3 h (>5 half-lives), the absorbance A_e was measured, and the equilibrium constant was determined as ($A_0 - A_e$)/A_e(0.034).

Error limits are reported as the standard deviation of five measurements under each set of conditions.

Addition of Methyl Isocyanide to (μ-H)$_2$Ru$_3$(CO)$_8$(μ-P(*t*-Bu)$_2$)$_2$. Two equivalents of methyl isocyanide were added to 10 mg of (μ-H)$_2$Ru$_3$(CO)$_8$(μ-P(*t*-Bu)$_2$)$_2$ in a NMR tube. An immediate color change from purple to orange occurred. Multiple products which could not be characterized were evident in the NMR spectrum.

Addition of P(OMe)$_3$ and PMe$_2$Ph to (μ-H)$_2$Ru$_3$(CO)$_8$(μ-P(*t*-Bu)$_2$)$_2$. One equivalent of the phosphine was added to 30 mg of (μ-H)$_2$Ru$_3$(CO)$_8$(μ-P(*t*-Bu)$_2$)$_2$ in a Schlenk flask under argon. An immediate color change from purple to red occurred. Multiple products which could not be characterized were indicated in the NMR spectrum.

Synthesis of (μ-D)$_2$Ru$_3$(CO)$_8$(μ-P(*t*-Bu)$_2$)$_2$. (μ-H)$_2$Ru$_3$(CO)$_8$(μ-P(*t*-Bu)$_2$)$_2$ (50 mg) was dissolved in hexanes (50 mL) in a Schlenk flask, and the solution was stirred for 10 min at 30 °C under 1 atm of deuterium gas (Matheson, CP grade, 99.5% isotopic purity). The reaction was reversed by stirring under nitrogen for 2 h. This procedure was repeated 5−7 times, until greater than 90% deuterium content was indicated by ^{1}H NMR spectroscopy.

Synthesis of (μ-H)$_2$Ru$_3$(CO)$_8$(μ-PCyc$_2$)$_2$ and (μ-H)Ru$_3$(CO)$_7$(μ-PCyc$_2$)$_3$. Ru$_3$(CO)$_{12}$ (300 mg) and HPCyc$_2$, Cyc = cyclohexyl (2.5 equiv), were added to 50 mL of dibutyl ether in a three-necked flask fitted with a nitrogen gas inlet and a reflux condenser. The suspension was heated at 100 °C for 1 h. After removal of the solvent, the resulting orange residue was extracted with 10 mL of hexanes and filtered. Purification by column chromatography on alumina yielded three bands as follows: yellow, Ru$_3$(CO)$_{12}$, 22 mg; orange, (μ-H)$_2$Ru$_3$(CO)$_8$(μ-PCyc$_2$)$_2$, 32 mg; orange, (μ-H)Ru$_3$(CO)$_8$(μ-PCyc$_2$)$_3$, 16 mg.

(μ-H)$_2$Ru$_3$(CO)$_8$(μ-PCyc$_2$)$_2$: IR(C_6H_{14}): 2069 m, 2033 s, 2020 s, 2003 ms, 1991 w, 1976 m, 1965 m cm^{-1}. ^{1}H NMR ($CDCl_3$, 290 K): 1.5−2.5 (m, 44H, C_6H_{11}), −17.53 (t, 2H, J_{PH} = 20.6 Hz) ppm. ^{31}P-{^{1}H} NMR ($CDCl_3$, 290 K): 211.92 (s, 2P) ppm. FAB-MS: *m*/*z* = 926 (^{102}Ru$_3$).

(μ-H)Ru$_3$(CO)$_7$(μ-PCyc$_2$)$_3$: IR (C_6H_{14}): 2044 m, 2002 s, 1995 s, 1980 m, 1939 m cm^{-1}. ^{1}H NMR ($CDCl_3$, 290 K): 1.5−2.5 (m, 66H, C_6H_{11}), −18.45 (dt, 1H, J_{PaH} = 19.2 Hz, J_{PbH} = 14.8 Hz) ppm. ^{31}P-{^{1}H} NMR ($CDCl_3$, 290 K): 200.0 (s, 2P$_a$), 181.2 (s, 1P$_b$) ppm. FAB-MS: *m*/*z* = 1094 (^{102}Ru$_3$). Anal. Calcd for $C_{43}H_{67}O_7P_3Ru_3$: C, 46.99, H, 6.10. Found: C, 46.02, H, 6.06.

Attempted Reaction of (μ-H)$_2$Ru$_3$(CO)$_8$(μ-*t*-Bu$_2$P)$_2$ with Benzyl Bromide. To a solution of 10 mg (0.012 mmol) of (μ-H)$_2$Ru$_3$(CO)$_8$-(μ-*t*-Bu$_2$P)$_2$ in 10 mL of hexanes under a nitrogen atmosphere was added 1 equiv of benzyl bromide. After 30 min no change in the color of

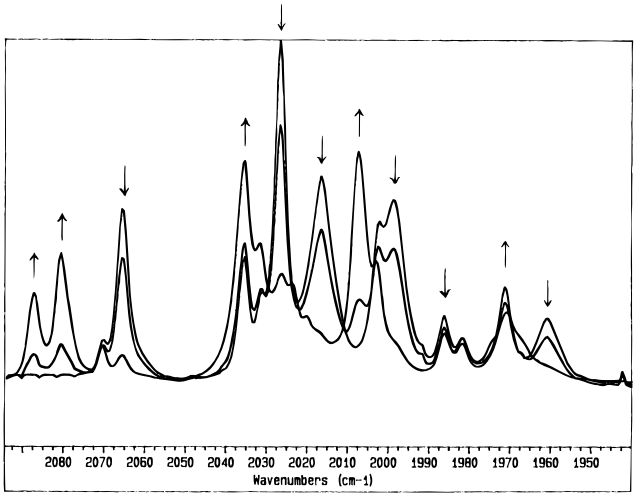

Figure 2. Infrared spectra during conversion of $(\mu\text{-H})_2Ru_3(CO)_8(\mu\text{-P}(t\text{-Bu})_2)_2$ to $(\mu\text{-H})_2(H)_2Ru_3(CO)_8(\mu\text{-P}(t\text{-Bu})_2)_2$.

the solution nor in the IR spectrum had occurred. The cluster was recovered in nearly quantitative yield.

Attempted Reaction of $(\mu\text{-H})_2Ru_3(CO)_8(\mu\text{-}t\text{-Bu}_2P)_2$ with $HSnBu_3$. To a solution of 10 mg (0.012 mmol) of $(\mu\text{-H})_2Ru_3(CO)_8(\mu\text{-P}(t\text{-Bu})_2)_2$ in 10 mL of hexanes under a nitrogen atmosphere was added 1 equiv (5 μL) of $HSnBu_3$. After 30 min no change in the color of the solution nor the IR spectrum had occurred. The cluster was recovered in nearly quantitative yield.

^{13}CO Exchange of $(\mu\text{-H})_2Ru_3(CO)_8(\mu\text{-PR}_2)_2$, R = *t*-Bu and Cyc. A solution of $(\mu\text{-H})_2Ru_3(CO)_8(\mu\text{-P}(t\text{-Bu})_2)_2$ (10 mg) in 10 mL of hexanes was placed in a jacketed reaction vessel, thermostatted at 30.0 °C. The IR spectrum of the solution was recorded, and then the solution was saturated with ^{13}CO (99% ^{13}C, 10% ^{18}O). An IR spectrum was immediately recorded. After 5 min a sample was taken for IR analysis, which showed a major reduction in the intensities of several absorptions in the CO stretching region. The solution was evaporated to dryness. The residue was submitted for analysis by mass spectroscopy (FAB). Mass spectra of enriched and natural abundance samples display an isotope multiplet of low intensity assigned to the $(M - C_4H_9)^+$ ion. ^{13}C enrichment was determined by a best fit of the experimental isotope multiplet for the $(M - C_4H_9)^+$ ion to a computer calculated theoretical ion based upon random exchange of eight CO ligands with enriched CO (99% ^{13}C, 10% ^{18}O). The fitting program MSCALC, is a home-written modification of MASSPAN.[16] The best fit was obtained for 60% enrichment. A ^{13}C NMR spectrum of this product, taken 24 h after the initial exposure showed that the label was randomly distributed among the eight CO ligands: ($CDCl_3$, 20 °C) 205.1 (br, 2C), 200.9 (s, 2C), 200.6 (br, 2C), and 195.8 (br, 2C).

An identical experiment was performed with $(\mu\text{-H})_2Ru_3(CO)_8(\mu\text{-PCyc}_2)_2$. After 18 h no change in the IR spectrum was noted.

Results

In hydrocarbon solution, $(\mu\text{-H})_2Ru_3(CO)_8(\mu\text{-P}(t\text{-Bu})_2)_2$ reacts quantitatively with hydrogen at 1 atm and 20−40 °C to give $(\mu\text{-H})_2Ru_3(H)_2(CO)_8(\mu\text{-P}(t\text{-Bu})_2)_2$ (Figure 1). This reaction could be quantitatively reversed by flushing with nitrogen or argon at 1 atm and 10−30 °C. An isobestic point is noted in the terminal carbonyl region of the infrared spectrum, implying that no measurable quantity of an intermediate is formed during the reaction (Figure 2).

The rate of hydrogenation of $(\mu\text{-H})_2Ru_3(CO)_8(\mu\text{-P}(t\text{-Bu})_2)_2$ at 1 atm and 20−40 °C was determined by monitoring the 532 nm absorption in the UV−vis spectrum. Plots of $\ln(A_t - A_\infty)$ vs time were linear, consistent with a rate law which is first-order in cluster concentration (Supporting Information, Figure 1S). Plots of k_{obs} at 20.0, 30.0, and 40.0 °C vs hydrogen partial pressure (0.1−1 atm hydrogen, balance nitrogen) were linear, signifying a rate law which is also first-order in hydrogen under these conditions (Supporting Information, Figure 2S; Table 1). The rate of hydrogenation is also strongly dependent upon the partial pressure of carbon monoxide. Above 0.1 atm carbon monoxide, the reaction was almost completely inhibited. Plots of $1/k_{obs}$ vs P_{CO}/P_{H_2} are linear with zero intercepts (Figure 3, Table 1), consistent with a rate law inverse order in P_{CO}. From an Eyring plot of $\ln(k_{obs}/T)$ vs $1/T$ the activation parameters for the hydrogenation under 1 atm of hydrogen were determined to be $\Delta H_F^{\ddagger} = 35(3)$ kJ/mol and $\Delta S_F^{\ddagger} = -158(10)$ J/mol-K (Supporting Information, Figure 3S). Rate constants were also obtained at 20−40 °C and under hydrogen containing various pressures of CO. Using data at P_{CO} greater than 0.07 atm, a plot of $\ln(k_{obs}P_{CO}/P_{H_2}T)$ vs $1/T$ provides $\Delta H^{\ddagger} = 115(12)$ kJ/mol and $\Delta S^{\ddagger} = +56(38)$ J/K-mol. The deuterium kinetic isotope effect was measured at 30 °C from the rate of hydrogenation of $(\mu\text{-H})_2Ru_3(CO)_8(\mu\text{-}t\text{-Bu}_2P)_2$ and the rate of deuteriation of $(\mu\text{-D})_2Ru_3(CO)_8(\mu\text{-}t\text{-Bu}_2P)_2$ under 1 atm of D_2 (99% isotopic purity), and the value of k_{obs}^H/k_{obs}^D was determined to be 1.30(0.09).

The rate of hydrogen elimination from $(\mu\text{-H})_2Ru_3(H)_2(CO)_8(\mu\text{-P}(t\text{-Bu})_2)_2$ under nitrogen and at 10−30 °C was determined by monitoring the 2081 cm^{-1} absorption of the infrared spectrum. Plots of ln(absorbance) vs time were linear (Supporting Information, Figure 4S), indicating a first-order depen-

Table 1. Rate Constants for $H_2 + (\mu\text{-H})_2Ru_3(CO)_8(\mu\text{-P}(t\text{-Bu})_2)_2 \rightarrow (\mu\text{-H})_2Ru_3(H)_2(CO)_8(\mu\text{-P}(t\text{-Bu})_2)_2$ at 1 atm Pressure in Heptane

T, °C	P_{H_2}, atm	P_{CO}, atm	P_{N_2}, atm	k_{obs}, s^{-1}
20.0	1	0	0	$1.99(0.014) \times 10^{-2}$
	0.986	0.014	0	$1.7(0.2) \times 10^{-2}$
	0.925	0.075	0	$2.1(0.2) \times 10^{-4}$
	0.537	0	0.463	$1.2(0.2) \times 10^{-2}$
	0.132	0	0.868	$2.3(0.4) \times 10^{-3}$
30.0	1	0	0	$3.4(0.4) \times 10^{-2}$
	0.986	0.014	0	$1.8(0.5) \times 10^{-2}$
	0.925	0.075	0	$8.3(0.9) \times 10^{-4}$
	0.771	0.229	0	$2.3(0.1) \times 10^{-4}$
	0.679	0.321	0	$1.6(0.1) \times 10^{-4}$
	0.537	0	0.463	$2.0(0.3) \times 10^{-2}$
	0.132	0	0.868	$5.0(0.3) \times 10^{-3}$
40.0	1	0	0	$5.5(0.5) \times 10^{-2}$
	0.986	0.014	0	$3.9(0.2) \times 10^{-2}$
	0.925	0.075	0	$3.9(0.2) \times 10^{-3}$
	0.771	0.229	0	$8.1(0.1) \times 10^{-4}$
	0.679	0.321	0	$4.8(0.3) \times 10^{-4}$
	0.537	0	0.463	$2.9(0.8) \times 10^{-2}$
	0.132	0	0.868	$6(2) \times 10^{-3}$

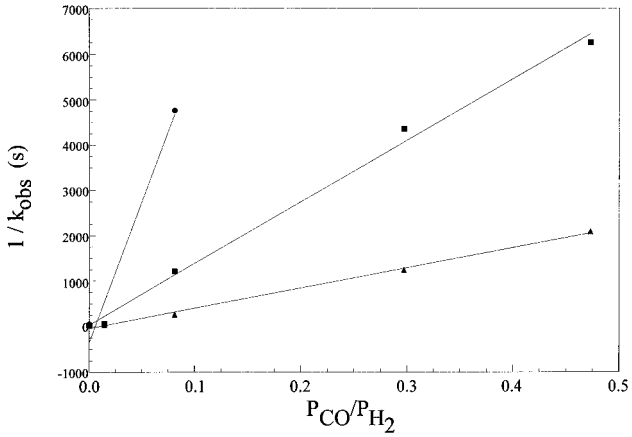

Figure 3. Plot of $1/k_{obs}$ vs $P(CO)/P(H_2)$ for hydrogenation of $(\mu\text{-H})_2Ru_3(CO)_8(\mu\text{-P}(t\text{-Bu})_2)_2$ at 20.0, 30.0, and 40.0 °C and 1 atm.

(15) Program KINPLOT, written by Dr. R. Rusczcyk and locally modified.

(16) Andrews, M. A. Ph.D. Dissertation; UCLA, Los Angelos, CA, 1977.

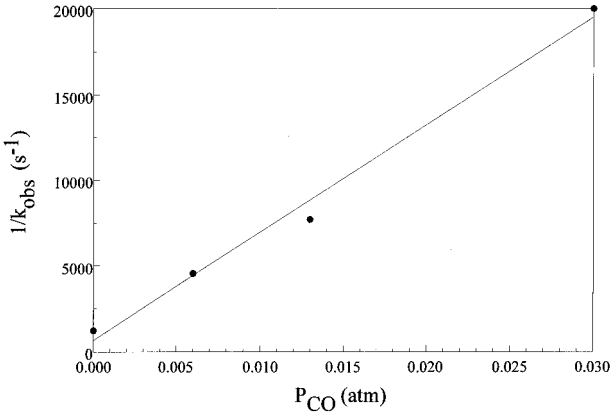

Figure 4. Plot of $1/k_{obs}$ vs P(CO) for hydrogen loss from $(\mu\text{-H})_2(\text{H})_2\text{Ru}_3(\text{CO})_8(\mu\text{-P}(t\text{-Bu})_2)_2$ at 30.0 °C.

Table 2. Rate Constants for $(\mu\text{-H})_2\text{Ru}_3(\text{H})_2(\text{CO})_8(\mu\text{-P}(t\text{-Bu})_2)_2 \rightarrow \text{H}_2 + (\mu\text{-H})_2\text{Ru}_3(\text{CO})_8(\mu\text{-P}(t\text{-Bu})_2)_2$

T, °C	solvent	P_{CO}, atm	P_{N_2}, atm	k_{obs}, s^{-1}
10.0	decane	0	1	$4.40(0.08) \times 10^{-5}$
20.0	decane	0	1	$1.75(0.29) \times 10^{-4}$
30.0	decane	0	1	$7.2(0.4) \times 10^{-4}$
30.0	heptane	0	1	$8.1(0.3) \times 10^{-4}$
30.0	heptane	0.006	0.994	$2.2(0.2) \times 10^{-4}$
30.0	heptane	0.013	0.987	$1.30(0.03) \times 10^{-4}$
30.0	heptane	0.03	0.97	$5.0(0.2) \times 10^{-5}$
30.0	THF	0	1	$1.01(0.05) \times 10^{-3}$

Table 3. Equilibrium Constants for $\text{H}_2(\text{g}) + (\mu\text{-H})_2\text{Ru}_3(\text{CO})_8(\mu\text{-P}(t\text{-Bu}_2))_2(\text{soln}) \rightarrow (\mu\text{-H})_2(\text{H})_2\text{Ru}_3(\text{CO})_8(\mu\text{-P}(t\text{-Bu})_2)_2$ (soln) under 0.034 atm Hydrogen

T, °C	solvent	K_{eq}, atm^{-1}
0.0	heptane	500(4)
10.0	heptane	235(6)
20.0	heptane	99(4)
30.0	heptane	56(3)
40.0	heptane	33(4)
30.0	THF	134(8)

Table 4. Summary of Kinetic and Thermodynamic Data

$\Delta H°$ −49.1(3.7) kJ/mol, based on H_2 atm	$\Delta S°$ −128(12) J/mol·K, based on H_2 atm
$\Delta H_F^{\ddagger}$ 35(3) kJ/mol, based on H_2 atm	$\Delta S_F^{\ddagger}$ −158(10) J/mol·K, based on H_2 atm
$\Delta H_R^{\ddagger}$ 97(3) kJ/mol	$\Delta S_R^{\ddagger}$ +15(12) J/mol·K
k_H/k_D 1.30(0.09), 30 °C, H_2 addition, H_2 atm	k_H/k_D 1.39(0.16) 30.0 °C, H_2 loss, N_2 atm
k_2/k_1k_3 (30.0 °C) $1.40(0.11) \times 10^4$ s	k_5/k_4k_6 (30.0 °C) $6.3(0.9) \times 10^5$ s·atm^{-1}
K_{eq} 56(3) atm^{-1} at 30.0 °C	

dence upon cluster concentration. The rate of hydrogen loss is dependent on the partial pressure of carbon monoxide. Partial pressures of carbon monoxide above 0.1 atm almost completely inhibited the reaction. A plot of $1/k_{obs}$ vs P_{CO} is linear, with a slope of $6.3(0.9) \times 10^5$ atm^{-1}-s and an intercept of statistically indistinguishable from zero (600(1600) s) (Figure 4, Table 2) at 30.0 °C. From an Eyring plot of $\ln(k_{obs}/T)$ vs $1/T$ the apparent activation parameters for the loss of hydrogen under nitrogen were determined to be $\Delta H_R^{\ddagger} = 97(3)$ kJ/mol (23.2(0.8) kcal/mol) and $\Delta S_R^{\ddagger} = +15(12)$ J/mol-K (+3.6(1.4) cal/mol-K) (Supporting Information, Figure 5S). The deuterium kinetic isotope effect was measured at 30 °C from the rate of dehydrogenation of $(\mu\text{-H})_2(\text{H})_2\text{Ru}_3(\text{CO})_8(\mu\text{-P}(t\text{-Bu})_2)_2$ and the rate of deuterium loss from $(\mu\text{-D})_2(\text{D})_2\text{Ru}_3(\text{CO})_8(\mu\text{-P}(t\text{-Bu})_2)_2$ (>90% isotopic purity by ^{1}H NMR) under nitrogen, and the value of k_{obs}^{H}/k_{obs}^{D} was determined to be 1.39(0.16).

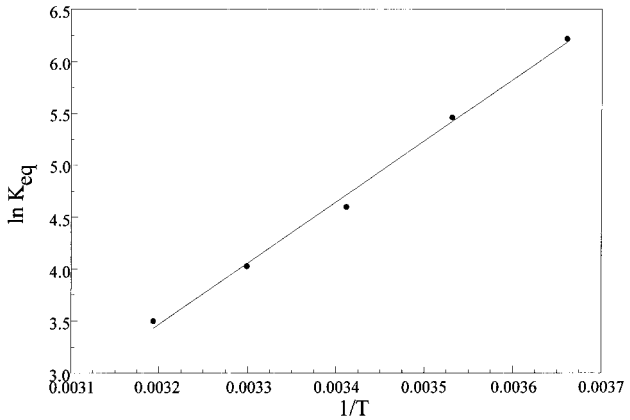

Figure 5. Plot of $\ln(K_{eq})$ vs $1/T$ for $\text{H}_2(\text{g}) + (\mu\text{-H})_2\text{Ru}_3(\text{CO})_8(\mu\text{-P}(t\text{-Bu}_2))_2(\text{heptane}) \rightarrow (\mu\text{-H})_2(\text{H})_2\text{Ru}_3(\text{CO})_8(\mu\text{-P}(t\text{-Bu})_2)_2$ (heptane).

The equilibrium constant, K_{eq}, has been determined from the spectroscopically determined equilibrium concentrations of $(\mu\text{-H})_2\text{Ru}_3(\text{CO})_8(\mu\text{-P}(t\text{-Bu})_2)_2$ and $(\mu\text{-H})_2(\text{H})_2\text{Ru}_3(\text{CO})_8(\mu\text{-P}(t\text{-Bu})_2)_2$. Under a hydrogen partial pressure of 0.034 atm, the value of K is 56(3) atm^{-1} at 30.0 °C. The equilibrium constant was also determined at temperatures from 0.0 to 40.0 °C (Table 3). From a plot of $\ln(K_{eq})$ vs $1/T$ values of $\Delta H°$ −49.1(3.7) kJ/mol and $\Delta S°$ −128(12) J/K-mol were determined (Figure 5). The equilibrium constants at 30° (in heptane and in THF, 34 and 152 atm^{-1}, respectively) and the rate constants for the elimination of hydrogen (7.2×10^{-4} and 1.0×10^{-3} s^{-1}, respectively) are not significantly affected by the change of solvent.[37]

The new cluster $(\mu\text{-H})_2\text{Ru}_3(\text{CO})_8(\mu\text{-PCyc}_2)_2$ was prepared by the procedure used for the di-*tert*-butylphosphido analog. The spectroscopic data are entirely analogous to those for $(\mu\text{-H})_2\text{Ru}_3(\text{CO})_8(\mu\text{-PR}_2)_2$, R = Ph[14] and *t*-Bu.[13] The clusters $(\mu\text{-H})_2\text{Ru}_3(\text{CO})_8(\mu\text{-PPh}_2)_2$ and $(\mu\text{-H})_2\text{Ru}_3(\text{CO})_8(\mu\text{-PCyc}_2)_2$ do not react with hydrogen under the conditions examined. Also, no ^{13}CO exchange was found for $(\mu\text{-H})_2\text{Ru}_3(\text{CO})_8(\mu\text{-PCyc}_2)_2$ at 25° over an 18 h period.

Reactions of Lewis bases CNMe, P(OMe)_3, PMe_2Ph, and PPh_3 with $(\mu\text{-H})_2\text{Ru}_3(\text{CO})_8(\mu\text{-}t\text{-Bu}_2\text{P})_2$ were examined. Although rapid reactions occurred for CNMe, PMe_2Ph, and P(OMe)_3 at room temperature, numerous products were formed, none of which could be characterized. No reaction occurred with PPh_3.

Discussion

As one of the most fundamental of all reactions in organometallic chemistry, oxidative addition of molecular hydrogen (and the microscopic reverse, reductive elimination) has been the subject of many studies.[1] By comparison to the large number of studies of kinetics and mechanism of oxidative addition of hydrogen to monometallic complexes, few studies of oxidative additions by metal clusters have appeared.

In almost all examples hydrogen addition to a metal carbonyl cluster is preceded by ligand dissociation. One well-characterized example is the reaction of hydrogen with $\text{Os}_3(\text{CO})_{12-n}(\text{NCMe})_n$, $n = 1, 2$, which occurs by a NCMe dissociation and then hydrogen addition through what is proposed to be three-center synchronous process.[7b] Other examples of hydrogen addition following ligand dissociation and for which kinetic data are available include oxidative addition on $\text{H}_4\text{Ru}_4(\text{CO})_{12}$,[8] $[\text{Ru}_3(\text{CO})_{11}(\text{CO}_2\text{Me})]^{1-}$,[9] and $(\mu\text{-H})\text{Ru}_{3-n}\text{Os}_n(\mu\text{-COMe})(\text{CO})_{10}$.[5]

Kinetics of reductive elimination of hydrogen provide more information concerning the nature of the hydrogen-cluster activated complex since the rate-determining step is usually hydrogen elimination. Reductive elimination of hydrogen from

$(\mu\text{-H})_3\text{Ru}_{3-n}\text{Os}_n(\mu_3\text{-COMe})(\text{CO})_9$, $n = 0-3$, has been the subject of several studies.[5] The variation in the rate of hydrogen elimination with mixed metal composition suggests that the mechanism involves migration of two bridging hydrides to terminal coordination sites on a single metal atom, followed by reductive elimination through a synchronous, three-center transition state. Kinetics of reductive elimination of hydrogen from $(\mu\text{-H})_2\text{Os}_3(\text{CO})_{10}$,[7a] $\text{H}(\mu\text{-H})\text{Os}_3(\text{CO})_{11}$,[7a] and $\text{H}(\mu\text{-H})\text{Ru}_3(\text{CO})_{11}$[6] have been reported. In each case, rate-determining hydrogen elimination is followed by ligand association. Deuterium kinetic isotope effects are small, 1.2−2, and consistent with the proposed mechanism.

Very few examples of hydrogen addition to a cluster without ligand dissociation have been studied. Casey and co-workers very recently reported a kinetic study of the addition of hydrogen to the unsaturated cluster $\text{Cp*}_3\text{Co}_3(\mu_3\text{-H})(\mu_3\text{-CMe})$ and reductive elimination from the product $\text{Cp*}_3\text{Co}_3(\mu\text{-H})_3(\mu_3\text{-CMe})$.[11] Other examples of unsaturated polynuclear complexes which add hydrogen include $\text{Cp*}_3\text{Rh}_2\text{M}(\mu\text{-CO})_2$ (M = Rh, Ir),[17] $\text{Cp*}_3\text{Co}_3(\mu_3\text{-CO})_2$,[18] $\text{Os}_3\text{Pt}(\mu\text{-H})_2(\text{CO})_{10}(\text{PCyc}_3)$,[19] and $\text{CoRh}(\text{CO})_7$.[10] Hydrogen additions across metal−metal multiple bonds have been reported for $\text{Ta}_2\text{Cl}_6(\text{PMe}_3)_4$,[20] $\text{W}_2(\eta^5\text{-C}_5\text{H}_4\text{R})_2\text{Cl}_4$,[21] and $\text{RuMo}(\text{CO})_5(\text{dppm})_2$,[22] but to our knowledge kinetic studies of these systems have not been performed. Qualitative MO theory was used to show that intramolecular dinuclear 1,2-reductive eliminations are symmetry forbidden and should have a large activation barrier for concerted least-motion pathway; oxidative additions should be somewhat more favorable.[23]

Few examples in which hydrogen addition follows cleavage of a single metal−metal bond, rather than ligand dissociation, have appeared. Kinetics of hydrogen addition across the Cr−Cr bond of $[\text{Cr}(\text{CO})_3\text{C}_5\text{H}_4]_2\text{CH}_2$, forming $[\text{HCr}(\text{CO})_3\text{C}_5\text{H}_4]_2\text{CH}_2$ have been studied.[11] Hydrogen addition across the Rh−Rh single bond of $[\text{Rh}(\text{OEP})]_2$ occurs by homolytic cleavage of the Rh−Rh bond, followed by reaction of H_2 with two Rh radicals in what is proposed to be a four-center transition state.[24] Related examples are those for which the 17-electron metal complex is stable with respect to metal−metal bond formation.[4] For these reactions, the rate law is first-order in hydrogen and second-order in the metal radical. A classic example is hydrogen addition to $[\text{Co}(\text{CN})_5]^{3-}$, forming $[\text{HCo}(\text{CN})_5]^{3-}$. The activated complex has the composition $[\text{H}_2\text{Co}_2(\text{CN})_{10}]^{6-}$, and a termolecular mechanism with a four-center transition state has been proposed.[25] Hydrogen additions to (tetramesitylporphyrinato)Rh(II)[26] and to $\text{Co}(\text{dmgH})_2$[27] also appear to occur by this mechanism.

Two well-known examples of reductive elimination of hydrogen from mononuclear metal hydrides, with formation of a metal−metal bonded dinuclear complexes, are shown in eqs 1 and 2. Norton and co-workers found that eq 2 occurred by rate-determining CO dissociation.[28] A similar mechanism was suggested for eq 1,[29] but another study supports a radical mechanism involving $\text{Co}(\text{CO})_4$.[30] Binuclear reductive elimination, forming 17-electron metal complexes rather than a metal−metal bond, was found for $\text{HCo}(\text{dmgH})_2(\text{PBu}_3)$ in acidic solution; parallel homolytic and heterolytic cleavage of the Co−H bond was proposed.[31]

$$2\text{HCo}(\text{CO})_4 \rightarrow \text{H}_2 + \text{Co}_2(\text{CO})_8 \quad (1)$$

$$2\text{H}_2\text{Os}(\text{CO})_4 \rightarrow \text{H}_2 + \text{H}_2\text{Os}_2(\text{CO})_8 \quad (2)$$

The addition of hydrogen to $(\mu\text{-H})_2\text{Ru}_3(\text{CO})_8(\mu\text{-P}(t\text{-Bu}_2))_2$ is an intriguing subject for a kinetic investigation as one of the few reversible hydrogenations of trimetallic clusters, as a rare example of hydrogen addition across a metal−metal single bond and as a rare example of formation of a Group 8 trimetallic cluster with terminal hydride ligands. Possible mechanisms are as follows: (a) ligand dissociation, followed by oxidation addition at a single metal center; (b) metal−metal bond cleavage, followed by hydrogen addition to the two 17-electron metal centers via a four-center transition state; and (c) direct addition across the intact metal−metal bond through a four-center transition state. A less likely possibility is heterolytic cleavage of the H−H bond.

Our kinetic results are consistent with the following mechanism:

$$(\mu\text{-H})_2\text{Ru}_3(\text{CO})_8(\mu\text{-PR}_2)_2 \underset{k_2}{\overset{k_1}{\rightleftharpoons}} (\mu\text{-H})_2\text{Ru}_3(\text{CO})_7(\mu\text{-PR}_2)_2 + \text{CO} \quad (3)$$

$$(\mu\text{-H})_2\text{Ru}_3(\text{CO})_7(\mu\text{-PR}_2)_2 + \text{H}_2 \underset{k_4}{\overset{k_3}{\rightleftharpoons}} (\mu\text{-H})_2(\text{H})_2\text{Ru}_3(\text{CO})_7(\mu\text{-PR}_2)_2 \quad (4)$$

$$(\mu\text{-H})_2(\text{H})_2\text{Ru}_3(\text{CO})_7(\mu\text{-PR}_2)_2 + \text{CO} \underset{k_6}{\overset{k_5}{\rightleftharpoons}} (\mu\text{-H})_2(\text{H})_2\text{Ru}_3(\text{CO})_8(\mu\text{-PR}_2)_2 \quad (5)$$

Both oxidative addition and reductive elimination are proposed to proceed through a three-center transition state at a single metal site. The evidence in support of this will be described below.

The reductive elimination of hydrogen from $(\mu\text{-H})_2(\text{H})_2\text{Ru}_3(\text{CO})_8(\mu\text{-P}(t\text{-Bu}_2))_2$ involves reversible CO dissociation, followed by rate-determining loss of hydrogen. Under our experimental conditions, the rate of hydrogen elimination is given by eq 6:

$$\text{rate} = \frac{k_4k_6}{k_5P_{\text{CO}}}[\text{H}_4\text{Ru}_3(\text{CO})_8(\text{PR}_2)_2] \quad (6)$$

A plot of $1/k_{\text{obs}}$ vs P_{CO} yields $k_5/k_4k_6 = 6.3(0.9) \times 10^5$ s-atm^{-1} at 30.0 °C. From the value of k_{obs} in the absence of added CO and the value of k_5/k_4k_6, the effective equilibrium pressure of CO in 1.5 mM $\text{H}_4\text{Ru}_3(\text{CO})_8(\mu\text{-P}(t\text{-Bu}_2))_2$ at 30.0 °C is ca. 2×10^{-3} atm, for [CO] in solution of ca. 2×10^{-5} M, 1.3% dissociated. The kinetic isotope effect of 1.39 is very similar to values reported for hydrogen elimination from a single metal center and also to reductive eliminations involving bridging hydrides in other cluster systems.[1,2,5,6]

(17) Bray, A. C.; Green, M.; Hankey, D. R.; Howard, J. A. K.; Johnson, O.; Stone, F. G. A. *J. Organomet. Chem.* **1985**, *281*, C12.
(18) Casey, C. P.; Widenhoefer, R. A.; Hallenbeck, S. L.; Hayashi, R. K.; Gavney, J. A., Jr. *Organometallics* **1994**, *13*, 4720.
(19) Farrugia, L. J.; Green, M.; Hankey, D. R.; Orpen, A. G.; Stone, F. G. A. *J. Chem. Soc., Chem. Commun.* **1983**, 310.
(20) Sattleberger, A. P.; Wilson, R. B., Jr.; Huffman, J. C. *Inorg. Chem.* **1982**, *21*, 4179.
(21) Green, M. L. H.; Mountford, P. *J. Chem. Soc., Chem. Commun.* **1989**, 732.
(22) Chaudret, B.; Dahan, F.; Sabo, S. *Organometallics* **1985**, *4*, 1490.
(23) Trinquier, G.; Hoffmann, R. *Organometallics* **1984**, *3*, 370.
(24) Wayland, B. B. *Polyhedron* **1988**, *7*, 1545.
(25) (a) Halpern, J.; Pribanic, M. *Inorg. Chem.* **1970**, *9*, 2616. (b) Halpern, J. *Inorg. Chim. Acta* **1983**, *77*, L105. (c) De Vries, B. *J. Catal.* **1962**, *1*, 489.
(26) Wayland, B. B.; Ba, S.; Sherry, A. E. *Inorg. Chem.* **1992**, *31*, 148.
(27) Simandi, L. I.; Budo-Zahonyi, E.; Szeverenyi, Z.; Nemeth, S. *J. Chem. Soc., Dalton Trans.* **1980**, 276.
(28) (a) Evans, J.; Norton, J. R. *J. Am. Chem. Soc.* **1974**, *96*, 7577. (b) Norton, J. R. *Acc. Chem. Res.* **1979**, *12*, 139.
(29) Ungvary, F.; Marko, L. *J. Organomet. Chem.* **1969**, *20*, 205.
(30) Wegman, R. W.; Brown, T. L. *J. Am. Chem. Soc.* **1980**, *102*, 2494.
(31) Chao, T.-H.; Espenson, J. H. *J. Am. Chem. Soc.* **1978**, *100*, 129.

The reductive elimination is similar in kind to the bimolecular reductive elimination in eq 2[28] above, which proceeds by CO dissociation, followed by bimolecular H_2 elimination (with concomitant metal−metal bond formation) and then CO recombination. The difference for the trimetallic cluster is that the two metal centers are also linked through the third metal atom. It is interesting that the rate for eq 2 is unaffected by CO concentration, with $\Delta S^{\ddagger}$ of +24 J/K-mol and $k_{HH}/k_{DD} = 2.9(0.4)$. The nature of the hydrogen elimination step has not been elucidated.

The oxidative addition of hydrogen to $(\mu\text{-H})_2Ru_3(CO)_8(\mu\text{-P}(t\text{-Bu})_2)_2$ involves rate-limiting addition of molecular hydrogen, following rapid, reversible CO dissociation. The linearity of the plot of the initial rate at 20 °C vs P_{H_2} (no added CO) indicates a process which is first-order in the partial pressure of hydrogen under these conditions. From rates under hydrogen/carbon monoxide mixtures and at 20.0, 30.0, and 40.0 °C, plots of $1/k_{obs}$ vs P_{CO}/P_{H_2} are reasonably linear with intercepts which are statistically indistinguishable from zero, indicating a rate law inverse order in P_{CO}. Based upon the proposed mechanism, the rate of hydrogen addition is given by eq 7, assuming that the step represented by k_3 is rate-determining, that there is a rapid equilibrium for eq 3, that the reverse reaction is negligible, and that the concentration of CO is constant, either due to the establishment of a steady-state or due to maintaining a constant CO pressure from an external source. Derivation of the rate law for this mechanism under conditions where the reverse reaction is negligible and when no external source of CO is present (then the CO concentration is always equal to the concentration of the first intermediate, $[H_2Ru_3(CO)_7(\mu\text{-P}(t\text{-Bu})_2)_2]$) gives eq 8. This rate law does not apply under our experimental conditions as first-order plots display good linearity over greater than 3 half-lives, whereas half-order plots display curvature. Equation 8 is not applicable because CO dissociation from the product is not negligible at high conversion. Based upon the experimentally determined value of k_1k_3/k_2 of $7.1(0.9) \times 10^{-5}$ s^{-1} and the value of k_{obs} in the absence of added CO, the effective P_{CO} due to dissociation from $H_2Ru_3(CO)_8(\mu\text{-P}(t\text{-Bu})_2)_2$ is ca. 2×10^{-3} atm at 0.5 mM, giving a CO concentration of ca. 2×10^{-5} M, 4% dissociated. Based upon the experimentally determined value of k_5/k_4k_6 of $6.3(0.9) \times 10^5$ s-atm^{-1} and the value of k_{obs} for the reverse reaction in the absence of added CO, the effective P_{CO} due to dissociation from $H_4Ru_3(CO)_8(\mu\text{-P}(t\text{-Bu})_2)_2$ is ca. 2×10^{-3} atm at 1.5 mM, 1% dissociated. For a quantitative hydrogenation at 0.5 mM the equilibrium pressure of CO is calculated to decrease from 2×10^{-3} atm initially to 1×10^{-3} atm at 100% conversion, thus the pressure of CO does not change enough with conversion to allow for the detection of curvature in plots of ln(absorbance) vs time.

A plot of $\ln(k_1k_3P_{CO}/k_2P_{H_2}T)$ vs $1/T$ at P_{CO} greater than 0.07 atm provides estimates of $\Delta H_{1,2}^{\circ} + \Delta H_3^{\ddagger} = 115(12)$ kJ/mol and $\Delta S_{1,2}^{\circ} + \Delta S_3^{\ddagger} = +56(38)$ J/K-mol. A value of +70 J/K-mol would be expected if the entropy of activation were only due to the difference between the entropies of CO(g) and H_2(g) (198 and 130 J/K-mol, respectively, at 25 °C).

Since the effects of deuterium substitution upon the values of k_1 (CO dissociation) and k_2 (CO reassociation) are expected to be small, the measured deuterium isotope effect upon k_1k_3/k_2 is primarily due to k_3, and the value is consistent with oxidative addition at a single metal center, comparable to the value of 1.34 found for addition to $Os_3(CO)_{11}$.[7b]

$$\text{rate} = \frac{k_1k_3P_{H_2}}{k_2P_{CO}}[H_2Ru_3(CO)_8(PR_2)_2] \tag{7}$$

$$\text{rate} = k_3[H_2]\sqrt{\frac{k_1}{k_2}}\sqrt{[H_2Ru_3(CO)_8(PR_2)_2]} \tag{8}$$

Exchange of the carbonyl ligands of $(\mu\text{-H})_2Ru_3(CO)_8(\mu\text{-P}(t\text{-Bu})_2)_2$ with ^{13}CO in solution is rapid. Analysis of the mass spectrum of a sample taken after 5 min under 99% ^{13}CO showed 60% exchange. Since CO dissociation was rapid at room temperature, we expected that ligand substitution should also be rapid. Indeed, $(\mu\text{-H})_2Ru_3(CO)_8(\mu\text{-P}(t\text{-Bu})_2)_2$ reacted rapidly with CNMe, PMe_2Ph, and $P(OMe)_3$ at room temperature, but numerous products were observed, and the color change from purple to orange suggests cluster fragmentation rather than ligand substitution. Surprisingly, the cluster did not react with PPh_3 at room temperature, suggesting that the cluster's coordination shell is severely crowded.

The equilibrium constant K_{eq} for the hydrogenation reaction is given by

$$K_{eq} = \frac{k_1k_3k_5}{k_2k_4k_6} \tag{9}$$

Substitution of the values of k_1k_3/k_2 and k_5/k_4k_6 yields $K_{eq} = 46(8)$ atm^{-1} at 30.0 °C. We experimentally determined K_{eq} from concentrations of $(\mu\text{-H})_2Ru_3(CO)_8(\mu\text{-P}(t\text{-Bu})_2)_2$ and $(\mu\text{-H})_2Ru_3(H)_2(CO)_8(\mu\text{-P}(t\text{-Bu})_2)_2$ (measured by IR spectroscopy) after equilibration at 30.0 °C under 0.034 atm hydrogen; this value was 56(3) atm^{-1}.

The enthalpy and entropy for the overall reaction were determined from the temperature dependence of the equilibrium constant at 0−40 °C. A plot of $\ln(K_{eq})$ vs $1/T$ yields ΔH° −49(4) kJ/mol and ΔS° −128(12) J/K-mol (if both clusters have identical entropies, ΔS° for the reaction is −130 J/K-mol, due only to the entropy of hydrogen gas). These thermodynamic parameters are in reasonable agreement with values calculated from the forward and reverse activation parameters ($\Delta H_F^{\ddagger} - \Delta H_R^{\ddagger}$) = −60(6) kJ/mol and ($\Delta S_F^{\ddagger} - \Delta S_R^{\ddagger}$) = −175(22) J/K-mol) derived from Figures 3S and 5S. From these data, an estimate of the Ru−Ru bond strength can be made. The heats of solution of $(\mu\text{-H})_2Ru_3(CO)_8(\mu\text{-P}(t\text{-Bu})_2)_2$ and of $(\mu\text{-H})_2(H)_2Ru_3(CO)_8(\mu\text{-P}(t\text{-Bu})_2)_2$ are assumed to be the same. The enthalpy for the reaction is then represented by

$$\Delta H^{\circ} = -49 \text{ kJ/mol} \approx E(\text{H−H}) + E(\text{Ru−Ru}) - 2E(\text{Ru−H})$$

Values estimated for E(Ru−H) are 266−272 kJ/mol.[33,34] The value of E(H−H) is taken as 436 kJ/mol.[35] Using these data Ru−Ru bond energy is calculated to be 47−59 kJ/mol. For comparison, the values suggested for the Ru−Ru bond energy of $Ru_3(CO)_{12}$ range from 78 to 115 kJ/mol, depending upon the assumptions used in the factoring of the total energy between Ru−Ru and Ru−CO bond energies.[36]

The unusually facile reaction of $(\mu\text{-H})_2Ru_3(CO)_8(\mu\text{-P}(t\text{-Bu})_2)_2$ with hydrogen, compared with the complete lack of reactivity

(32) The mole fraction solubilities of H_2 and of CO in heptane solution at 25 °C are 6.859×10^{-4} and 17.24×10^{-4}, respectively. For dissolution of hydrogen in octane, $\Delta H^{\circ} = 4.0$ J/mol and $\Delta S^{\circ} = -47.0$ J/K-mol. Wilhelm, E.; Battino, R. *Chem. Rev.* **1973**, *73*, 1.

(33) Tilset, M.; Parker, V. D. *J. Am. Chem. Soc.* **1989**, *111*, 6711; **1990**, *112*, 2843.

(34) Belt, S. T.; Scaiano, J. C.; Whittlesey, M. K. *J. Am. Chem. Soc.* **1993**, *115*, 1921.

(35) Kerr, J. A.; Parsonage, M. J.; Trotman-Dickenson, A. F. In CRC Handbook of Chemistry and Physics, 54th ed.; Weast, R. C., Ed.; CRC: Cleveland, OH, 1973; p F200.

(36) Connor, J. A. In Transition Metal Clusters; Johnson, B. F. G., Ed.; Wiley: Chichester, 1980; Chapter 5.

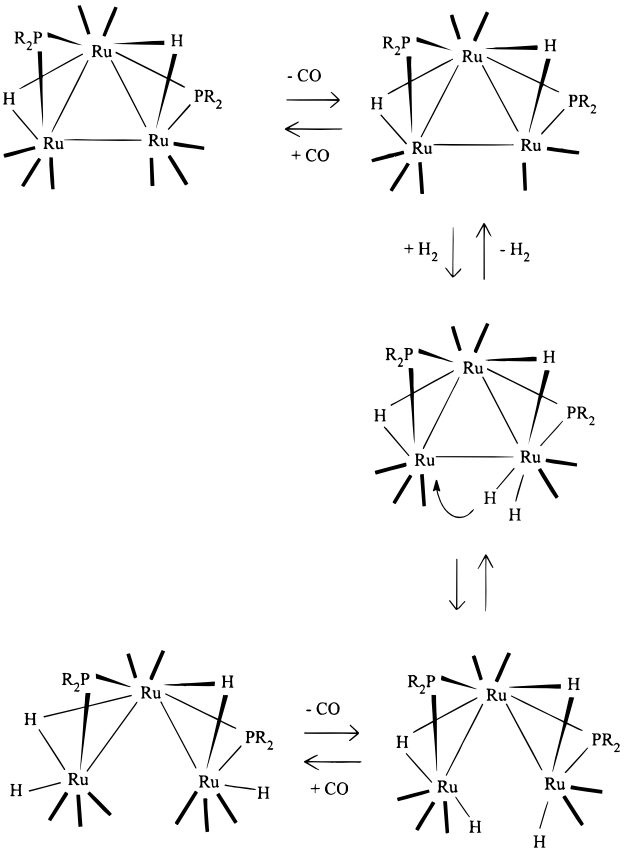

Figure 6. Pathway for hydrogen addition at a terminal Ru center.

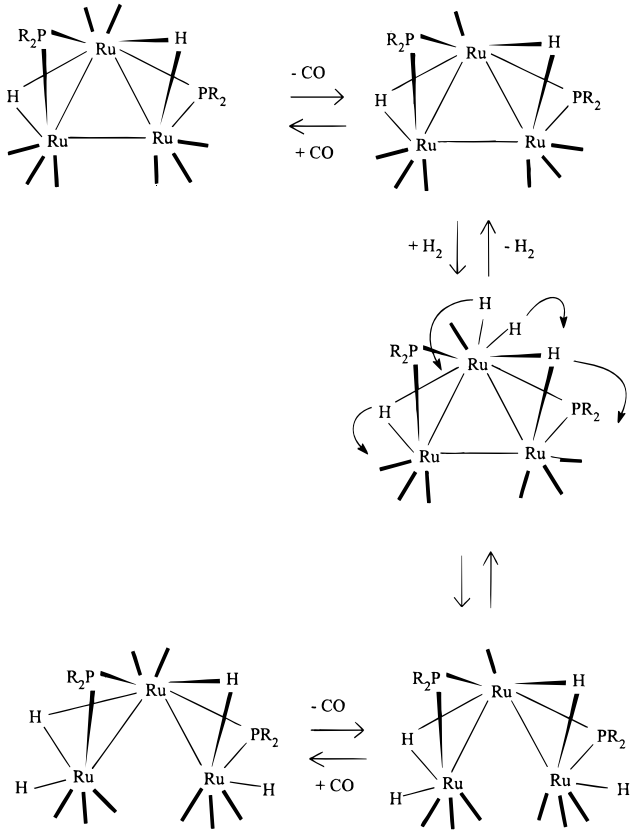

Figure 7. Pathway for hydrogen addition at the central Ru center.

exhibited by $(\mu\text{-H})_2Ru_3(CO)_8(\mu\text{-PR}_2)_2$, R = Cyc, Ph, suggests a steric factor weakening the Ru−Ru bond and also labilizing CO dissociation. X-ray structural determinations have been reported for $(\mu\text{-H})_2Ru_3(CO)_8(\mu\text{-P}(t\text{-Bu})_2)_2$[13] and $(\mu\text{-H})_2Ru_3(CO)_8(\mu\text{-PPh}_2)_2$.[14] The longer unbridged Ru−Ru bond for the former (3.046 Å vs 2.9464 Å) is structural evidence for the weakening of this bond, presumably due to steric interactions. Using the bond length/bond energy relationship proposed for $Ru_3(CO)_{12}$,[38] the corresponding unbridged Ru−Ru bond energies for $(\mu\text{-H})_2Ru_3(CO)_8(\mu\text{-PR}_2)_2$, R = *t*-Bu and Ph, are 57 and 67 kJ/mol, respectively (cf. 78 kJ/mol for $Ru_3(CO)_{12}$). The values obtained from the equilibrium data (47−59 kJ/mol) and from the bond length/bond energy relation are in reasonable agreement. Both analyses support an unusually weak Ru−Ru bond for $(\mu\text{-H})_2Ru_3(CO)_8(\mu\text{-P}(t\text{-Bu})_2)_2$. The UV−vis spectra of $(\mu\text{-H})_2Ru_3(CO)_8(\mu\text{-PR}_2)_2$ also support the relative Ru−Ru bond strengths. A detailed analysis of the electronic structure of $Ru_3(CO)_{12}$ attributed the absorption at 390 nm to the $\sigma \rightarrow \sigma^*$ transition associated with the metal−metal bond;[39] $(\mu\text{-H})_2Ru_3(CO)_8(\mu\text{-PR}_2)_2$, R = Ph and Cyc, display absorptions at 485 and 450 nm, respectively, whereas the di-*tert*-butylphosphido cluster has an absorption at 532 nm, consistent with a weaker Ru−Ru bond for the latter if these absorptions are due to $\sigma \rightarrow \sigma^*$ transitions.

We assume the primary factor responsible for the high reactivity of $(\mu\text{-H})_2Ru_3(CO)_8(\mu\text{-P}(t\text{-Bu})_2)_2$, compared with the complete lack of reactivity for $(\mu\text{-H})_2Ru_3(CO)_8(\mu\text{-P(Cyc)}_2)_2$ and $(\mu\text{-H})_2Ru_3(CO)_8(\mu\text{-PPh}_2)_2$, is steric in origin. The ability of the flatter cyclohexyl and phenyl groups (see the structure of $(\mu\text{-H})_2Ru_3(CO)_8(\mu\text{-PPh}_2)_2$[14]) to orient perpendicular to their geminal partners must make these sterically less demanding that the *tert*-butyl groups. The effects of conformational preferences upon variations in ligand cone angles have been noted.[40]

The weak Ru−Ru bond suggests the possibility that homolytic cleavage, forming a metal-centered biradical, might be involved. We have no direct evidence refuting this possibility. However, $(\mu\text{-H})_2Ru_3(CO)_8(\mu\text{-P}(t\text{-Bu})_2)_2$ does not react with benzyl bromide or $HSnBu_3$, substrates which typically react rapidly with radicals. Furthermore, previous studies of metal-centered biradicals have found negligible CO dissociation, and the biradicals undergo typical radical reactions such as recombination and halogen atom abstraction.[41] Many other 17-electron metal complexes undergo rapid associative ligand substitution, but lability for dissociative ligand substitution is uncommon.[42] For these reasons we consider the involvement of a biradical unlikely.

In summary, the data obtained in this study are consistent with the mechanism proposed in eqs 3−5. CO dissociation precedes both H_2 addition and elimination. The reaction is thermodynamically favored only because of an exceptionally weak Ru−Ru bond. The unusual weakness as well as exceptional lability for CO dissociation is attributed to steric strain associated with the bulky phosphido substituents. Despite the net cleavage of a metal−metal bond, hydrogen addition is proposed to occur at a single unsaturated Ru center. Two possible paths are shown in Figures 6 and 7. We are unable to specify the metal centers which are the sites of CO dissociation

(37) The estimated solubility of hydrogen in THF at 25 °C is 3.4 mM at 1 atm (ref 9), cf. 4.2 mM in octane (ref 32).

(38) The bond length (*d*)−enthalpy (*E*) relationship of the form $E = Ad^{-4.6}$, where $A = 1.522 \times 10^{13}$ pm$^{4.6}$kJ/mol, has been applied to $Ru_3(CO)_{12}$: Housecroft, C. E.; O'Neill, M. E.; Wade, K.; Smith, B. C. *J. Organomet. Chem*. **1981**, *213*, 35.

(39) (a) Knözinger, H. In Metal Clusters in Catalysis; Gates, B. C., Guczi, L., Knözinger, H., Eds.; Elsevier: Amsterdam, 1986; Section 6.3.1. (b) Tyler, D. R.; Levenson, R. A.; Gray, H. B. *J. Am. Chem. Soc*. **1978**, *100*, 7888.

(40) Brown, T. L.; Lee, K. J. *Coord. Chem. Rev*. **1993**, *128*, 89.

(41) Lee, K. W.; Hanckel, J. M.; Brown, T. L. *J. Am. Chem. Soc*. **1986**, *108*, 2266.

(42) *Organometallic Radical Processes*; Trogler, W. C., Ed.; Elsevier: Amsterdam, 1990; and references therein.

and hydrogen addition/elimination, since hydride and carbonyl mobility prevent site-specific labeling. Dissociation from one of the $Ru(CO)_3$ moieties and dihydrogen addition to this site can be followed by migration of one hydride to bridge to the adjacent $Ru(CO)_3$ moiety with no change in the electron count of the cluster; Ru−Ru bond cleavage could then generate the vacant coordination site required for CO coordination (Figure 6). This mechanism is attractive because the same Ru atom is involved in the Ru−Ru bond cleavage and CO reassociation. On the other hand (Figure 7), CO dissociation from the $Ru(CO)_2$ moiety and dihydrogen addition to this site can be followed by migration of the two hydrides to the bridging sites and the two bridging hydrides to terminal coordination sites on the $Ru(CO)_3$ centers with concomitant Ru−Ru bond cleavage to generate the vacant coordination site on the central Ru atom.[43] This mechanism is attractive because the central Ru center appears to be the msot sterically congested, because it accounts for the preference for the relief of steric strain by CO dissociation rather than Ru−Ru bond cleavage, and because it accounts for the orientations of the two terminal hydrides pointing away from each other in the product. However, by analogy to reductive elimination from $H_2Os(CO)_4$ (eq 2),[28] we favor the former mechanism (Figure 6).

Acknowledgment. This work was supported by the National Science Foundation through Grant CHE 92-13695. We thank Professor Richard Jones (University of Texas) for information concerning the syntheses and structures. Special thanks to A. Poë (University of Toronto) for an outstanding referee's critique.

(43) This mechanism was suggested by Professor A. Poë of the University of Toronto (private communication).

Note Added in Proof: A recent report (below) of $Ru_3(\mu\text{-}CO)(CO)_4(\mu_3\text{-}H)(\mu\text{-}H)(\mu\text{-}P(t\text{-}Bu)_2)_2(\mu\text{-}Ph_2PCH_2PPh_2)$, compositionally analogous to the unsaturated intermediate proposed in the hydrogenation reaction, provides evidence supporting the pathway in Figure 6 but suggests the possibility of hydride migration via a μ_3-H ligand. This compound does not react with hydrogen or with CO. Böttcher, H.-C.; Thönnessen, H.; Jones, P. G.; Schmutzler, R. *J. Organomet. Chem.* **1996**, *520*, 15.

Supporting Information Available: Figure 1S (plot of absorbance vs time for the hydrogenation of $(\mu\text{-}H)_2Ru_3(CO)_8(\mu\text{-}P(t\text{-}Bu)_2)_2$ at 30.0 °C and 1 atm), Figure 2S (plot of k_{obs} vs $P(H_2)$ for hydrogenation of $(\mu\text{-}H)_2Ru_3(CO)_8(\mu\text{-}P(t\text{-}Bu)_2)_2$ at 20.0 °C), Figure 3S (plot of $\ln(k_{obs}/T)$ vs 1/T for hydrogenation of $(\mu\text{-}H)_2Ru_3(CO)_8(\mu\text{-}P(t\text{-}Bu)_2)_2$ at 1 atm of hydrogen), Figure 4S (plot of absorbance vs time for the loss of hydrogen from $(\mu\text{-}H)_2(H)_2Ru_3(CO)_8(\mu\text{-}P(t\text{-}Bu)_2)_2$ at 30.0 °C), Figure 5S (plot of $\ln(k_{obs}/T)$ vs $1/T$ for hydrogen loss from $(\mu\text{-}H)_2(H)_2Ru_3(CO)_8(\mu\text{-}P(t\text{-}Bu)_2)_2$ under 1 atm of nitrogen) (6 pages). See any current masthead page for ordering and Internet access instructions.

JA9628819